

ON THE VARIANCE OF SEISMIC LOADS
TOWARD THE RELIABILITY-BASED DESIGN

M. Makino (I)
K. Matsumura (II)

Presenting Author: M. Makino

SUMMARY

The purpose of this paper is to investigate the variance of seismic loads. A theoretical seismic risk analysis, which is supported by observed data, and a corresponding simulation procedure are employed to estimate the coefficients of variation of lifetime maximum peak ground motions. The estimated values at four sites with various seismic activities along the Japanese Islands indicate the similar trend for the lifetime of 20 to 1000 years. The 100-year lifetime maximum values are estimated as about 0.6, 0.45 and 0.4 in displacement, velocity and acceleration, respectively.

INTRODUCTION

The rational evaluation of seismic loads is indispensable to practice the reliability-based design in Japan, one of the most seismic active regions of the world.

The seismic load is usually given in the form of response spectra which are related to the peak ground motions of strong earthquakes (Ref.1). A theoretical seismic risk analysis (Ref.2) based on a Poisson process and the truncated Gutenberg-Richter's magnitude law will reasonably lead to a probability distribution of the peak ground motions when an appropriate attenuation relation is provided. Gutenberg-Richter's law is conveniently applicable to almost all places in and near Japan. However, the seismic activity in Japan is so eminent that the effect of saturation in magnitude must be taken into consideration.

As a probability distribution of annual maximum peak ground motions, it seems to be better to use the type III extreme value distribution for a variate converted by a logarithmic transformation instead of the type II distribution, which is adopted in ANSI (Ref.3). Then the mean and the coefficient of variation of the peak ground motions in a certain probability level will be conveniently estimated by transformation of the variate.

SEISMIC RISK ANALYSIS AND SATURATION EFFECT IN MAGNITUDE

Most of great earthquakes in and near Japan have been found in subduction zones along the deep sea such as the Japan trench and the Nankai trough. As a matter of course active faults related to them are not yet well known in detail. In such a case the theoretical seismic risk may be evaluated from the risk of contributing areas with each individual activity. A near rectangular area divided by latitude and longitude in one degree is used as a unit area. The rate of earthquake occurrence, λ , of shallow earthquakes as great as and greater than magnitude 5 and the b -value in Gutenberg-Richter's law in the unit area are evaluated statistically from the earthquake catalogues during the period from 1951 to 1974 compiled by Japan Meteorological Agency.

-
- (I) Professor, Kyushu University, Fukuoka, Japan
(II) Associate professor, Kyushu University, Fukuoka, Japan

The upper bound, m_1 , of the maximum magnitude of earthquakes in each area is suggested by many investigators from historical earthquake documents and/or geological data. Provided the upper bound, m_1 , the theoretical probability distribution of annual maximum magnitudes in typical four regions shown in Fig.1 and Table 1 along the Japanese Islands can be obtained as in Fig.2(a)-(d). The solid line and dots in these figures are the theoretical and observed values, respectively. They are in good agreement and the saturation effect in magnitude is evident.

There are many attenuation relations expressing the peak ground motion, Y , with magnitude, M , and focal distance, R (km). Following three relations (Ref.4,5,6) for a horizontal component proposed in Japan are used in this study because the same definition of magnitude is satisfied.

$$\log(Y_d \cdot S.C.) = M - (3.13 + 1.83/R) - (1.66 + 3.60/R) \log(R) \quad (1-a)$$

$$\log(Y_v / 5\sqrt{T_g}) = 0.61M - (0.631 + 1.83/R) - (1.66 + 3.60/R) \log(R) \quad (1-b)$$

$$\log(Y_a) = 0.44M - 1.38 \log(R) - 1.04 \quad (\text{on stiff ground}) \quad (1-c)$$

where Y_d (cm), Y_v (kine) and Y_a (gal) are the peak amplitudes of displacement, velocity and acceleration respectively. $S.C.$ is the station correction factor and T_g (sec.) is the natural period of ground. The value of T_g is not so sensitive to the coefficients of variation of peak ground velocities that it is selected as 0.6(sec.), which stands for ordinary ground conditions in Japan. The focal depth of earthquakes is assumed to be 30 km in all cases.

The probability distributions of annual maximum peak ground displacements at four sites indicated in Fig.1 are obtained from the theoretical analysis as shown in Fig.3(a)-(d) with a solid line. Broken lines along the solid line are control curves with one standard deviation given by Eq.(3). The observed data, which are vectors of two horizontal peak components, are also shown in these figures as closed circles. Additional open circles are estimated data inversely from the attenuation relation for not obtained records due to limitation of seismographs. This comparison of the theoretical and observed results appears to support the procedure of this investigation.

The saturation effect in magnitude may be best illustrated by examples. The probability distributions of the annual maximum peak ground motion at a site in a moderately active homogeneous region for $\lambda=0.3$, $b=1.0$ in all contributing unit areas and the various levels of the upper bound, m_1 , of magnitude are shown in Fig.4 on logarithmic extremal probability paper. The type III extreme value distribution may be employed for the variate converted by a logarithmic transformation instead of the type II distribution which is expressed in a straight line on this paper.

CONTROL BAND

The basic hypotheses for the theoretical seismic risk analysis are considered as a character of a population. A Monte Carlo method may be employed as an alternate instead of the expectation calculation in the theoretical seismic risk analysis. The identical result may be obtained from the average of simulated samples if a sample size is adequate and a suitable plotting position is provided. 250 samples and Gringorten's proposal (Ref.7) with $a=0.33$ are used in this analysis. This plotting position may be adequately used when the shape parameter of the type III distribution is in the range of 3 to 6.

The probability distribution of central extremes in the annual peak ground motion can be asymptotically expected as a lognormal one because the type II distribution is realized under the condition that the saturation in magnitude is not considered. The probability distribution of the largest extremes may be also approximated as the lognormal one. Fig.5 indicates the frequency distribution in 20 intervals for 250 samples of the largest extremes, which are simulated with the truncated Gutenberg-Richter's law for a 1000-year observation period, lie in a straight line on logarithmic normal probability paper. It may be because the saturation effect in magnitude truncates the upper tail of the distribution that the above distribution is approximated as the lognormal distribution.

If the i -th extreme, Y_i , of the annual maximum peak ground motion is given as the lognormal distribution, the i -th extreme, Z_i , transformed by $Z = \log(Y)$ yields a normal distribution and its standard deviation, σ_{Z_i} , is expressed as (Ref.8),

$$\sigma_{Z_i} = \frac{\sqrt{G_Z(z_i)(1-G_Z(z_i))}}{g_Z(z_i)\sqrt{t}} \quad (2)$$

in which,

G_Z : probability distribution function,

g_Z : probability density function,

t : sample size (number of observation)

accordingly, the coefficient of variation of Y_i is expressed as,

$$V_{Y_i} = \sqrt{\exp(\sigma_{Z_i}^2 \ln(10))^2 - 1} \quad (3)$$

COEFFICIENT OF VARIATION OF THE MAXIMUM PEAK GROUND MOTIONS

The probability distribution of largest maxima closely depend on the upper tail of a parent distribution. The type III distribution may be applied to the theoretical one and/or equivalent simulated ordered data in the probability greater than 0.95 plotted on the logarithmic extremal probability paper. The three parameters of the type III distribution are easily obtained since the upper bound of the distribution is specified by the hypotheses. The three parameters at the four sites are determined as shown in Table 2.

The mean, μ_Z , and the standard deviation, σ_Z , of the transformed variate, Z , for the lifetime of n years are easily estimated by the stability postulate. Then, the mean, μ_Y , and the coefficient of variation, V_Y , of the peak ground motion at the four sites for the lifetime of n years are determined as shown in Fig.6. The differences in V_Y between the four sites are small while μ_Y is roughly proportional to the seismicity of the region. The coefficients of variation of the peak ground motions for the lifetime of 100 years are summarized in the first column of Table 3 as the average in the four sites.

According to Mohraz-Hall-Newmark study (Ref.9) the coefficients of variation of response amplification factors for a lightly damped system due to strong earthquakes are expressed as in the second column in this table. The values in these two columns are nearly comparable. If the peak ground motion and the amplification factor in response analysis are mutually independent, the coefficients of variation of peak response may be estimated as in the

third column in the Table 3.

CONCLUSION

It takes many years to establish a statistical sample such as ordered data of the annual maximum peak ground motion that is obtained from natural phenomena. One of the solution to avoid above difficulty is to use an appropriate simulation technique.

By using the theoretical seismic risk analysis and the simulation technique, the following results are obtained;

- 1) The frequency distribution of the largest extremes in the annual maximum peak ground motion may be approximated as a lognormal one.
- 2) The type III extreme value distribution on logarithmic extremal probability paper may be employed to express the probability distribution of the annual maximum peak ground motion.
- 3) The coefficients of variation of the 100-year lifetime maximum peak ground motions are nearly comparable to those of the response amplification factors due to strong earthquakes.

ACKNOWLEDGEMENT

The authors are deeply indebted to Mr. N. Tsuru and Mr. Y. Ikeda for their considerable assistance in preparing this manuscript. The calculation were carried out in the Computer Center of Kyushu University.

REFERENCES

- 1) Newmark, N.M. and Rosenblueth, E.: "Fundamentals of Earthquake Engineering", Prentice-Hall, N.Y., 1971
- 2) Cornell, C.A.: "Engineering Seismic Risk Analysis", B.S.S.A., Vol.58, 1968
- 3) "Building Code Requirements Design Loads in Buildings and Other Structures", ANSI A58, I-1972, American National Standards Institute, New York, N.Y., 1972
- 4) Makino, M. and Matsumura, K.: "A Correlation between the Recurrence Interval of Active Faults and the Extreme Value Distribution of Earthquake Ground Motion", Proc. of 5th Japan Earthquake Engineering Symposium, 1978
- 5) Kanai, K., Hirano, K. and Yoshizawa, S.: "Observation of Strong Earthquake Motion in Matsushiro Area : Part 1", Bull. Earthq. Res. Inst., Vol.44, 1966
- 6) Watabe, M. and Tohdo, M.: "Research on the Design Earthquake Ground Motions : Part-I", Trans. of Architectural Institute of Japan, Vol.303, 1981
- 7) Gringorten, I.I.: "A Plotting Rule for Extreme Probability Paper", J. of Geophysical Research, Vol.69, No.3, 1963
- 8) Gumbel, E.J.: "Statistics of Extremes", Columbia Univ. Press, 1958
- 9) Newmark, N.M., Blume, J.A. and Kapur, K.K.: "Seismic Design Spectra for Nuclear Power Plants", J. of Power Division, ASCE, 1973

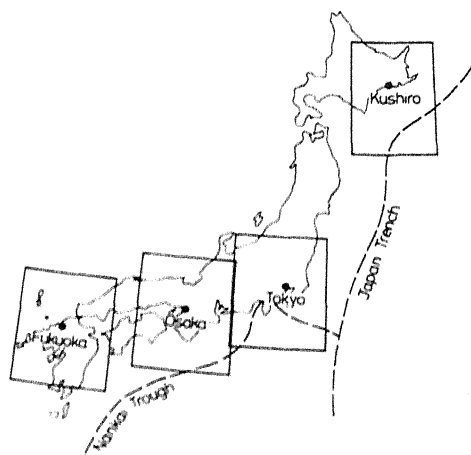


Fig. 1 Regions and sites of observation

Table 1. Statistical properties of four sites

site	$\Sigma\lambda$	\bar{b}	\bar{m}_1	$m_{1,s}$	S.C.
Fukuoka	3.24	1.27	7.50	7.00	1.00
Osaka	3.11	0.99	8.02	7.75	0.79
Tokyo	10.27	1.42	7.94	7.75	0.71
Kushiro	14.56	0.94	8.00	8.50	1.20

$\Sigma\lambda$: summation of rate of earthquake occurrence in the region
 \bar{b} : average of b -value in the region
 \bar{m}_1 : average of the upper bound of magnitude in the region
 $m_{1,s}$: upper bound of magnitude in the unit area where the site is located
S.C.: station correction factor for displacement

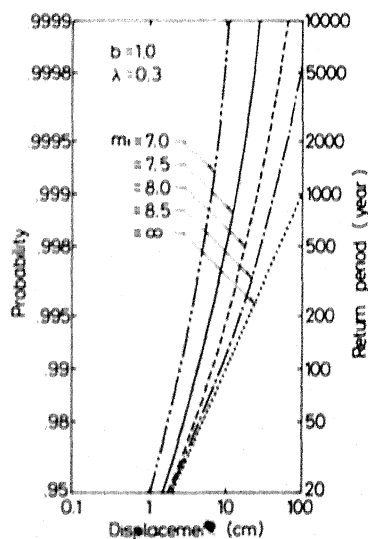
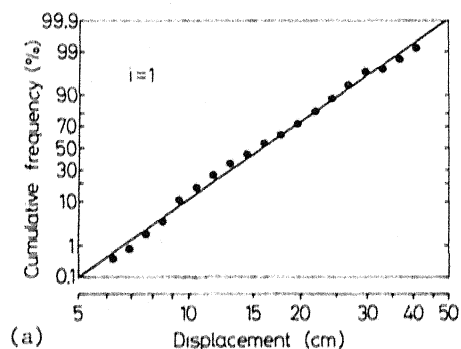
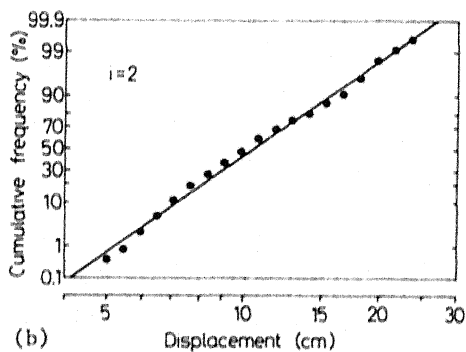


Fig. 4 Saturation effect in magnitude at a homogeneous region

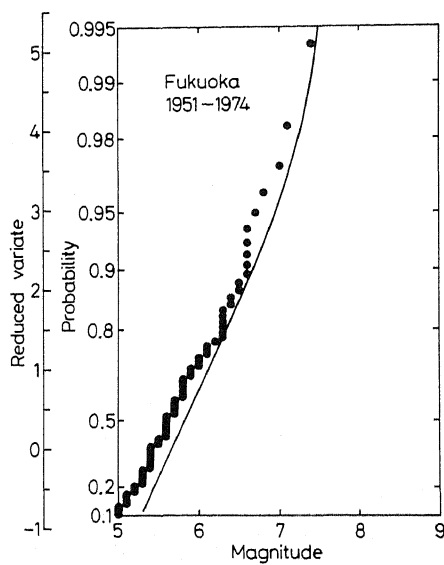


(a)

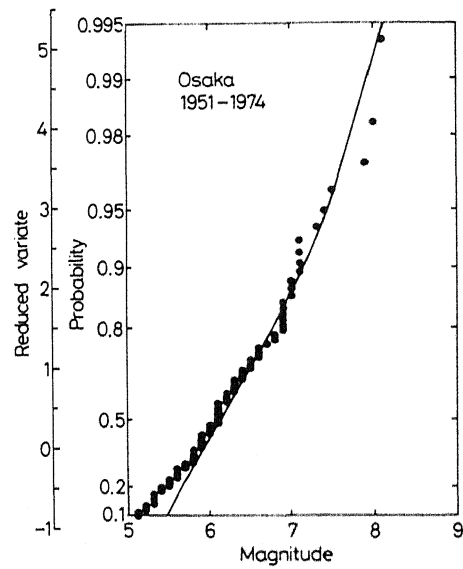


(b)

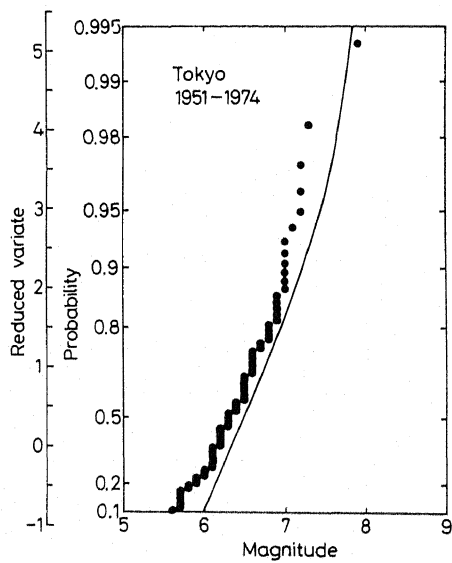
Fig. 5 Frequency distributions of the largest extremes on logarithmic normal probability paper



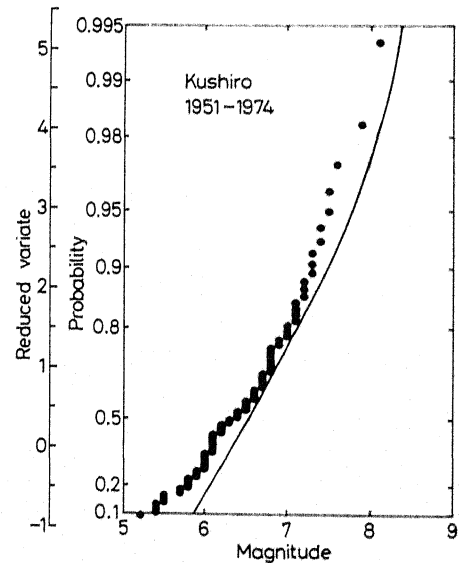
(a)



(b)



(c)



(d)

Fig. 2 Probability distributions of annual maximum magnitude;
solid line : theoretical , ● : observed data

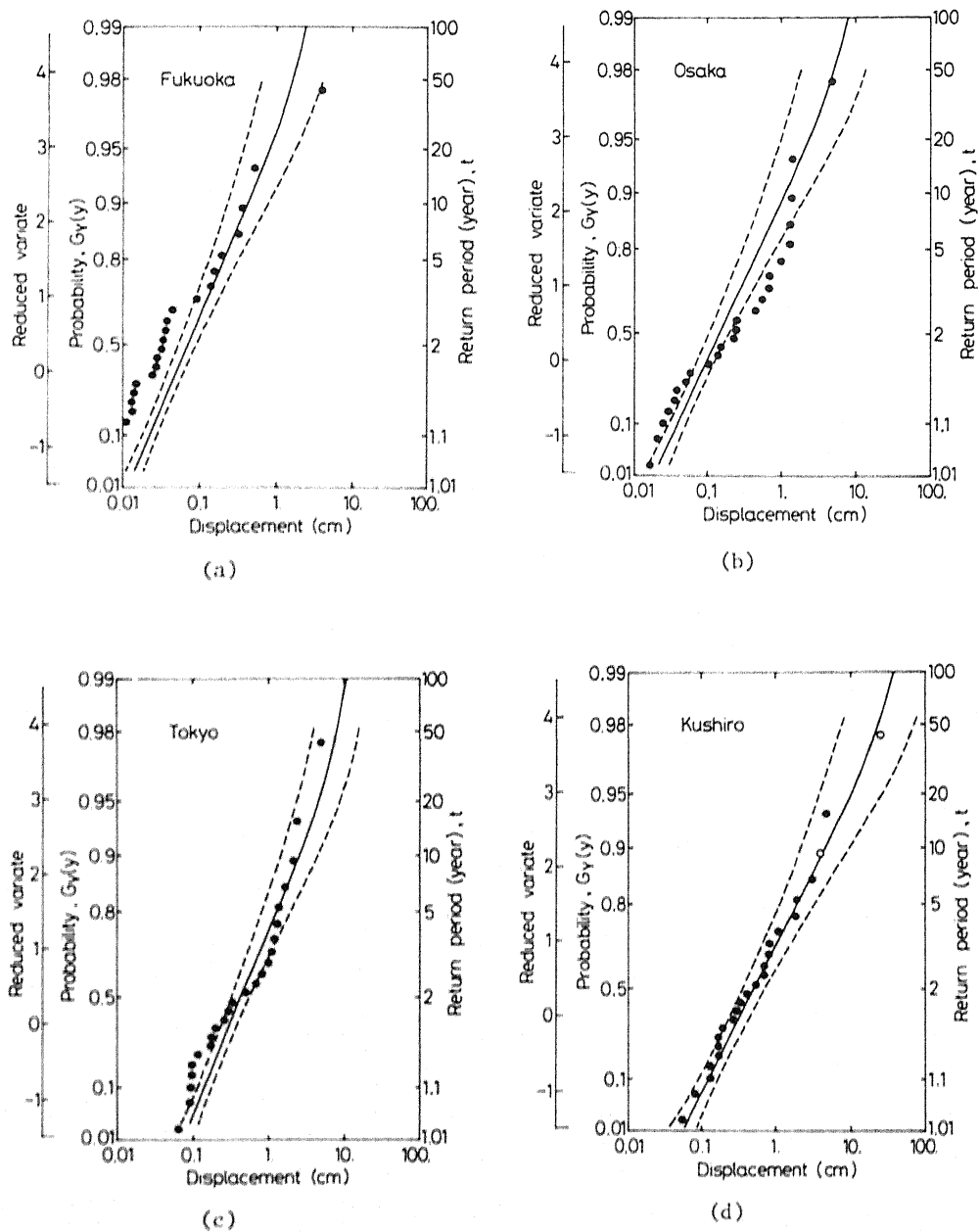


Fig. 3 Probability distributions of annual maximum displacements
 solid line:theoretical, broken lines:control curves,
 ● and ○ :observed and estimated data

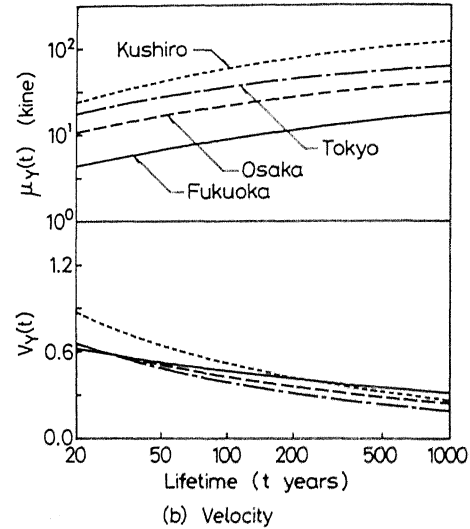
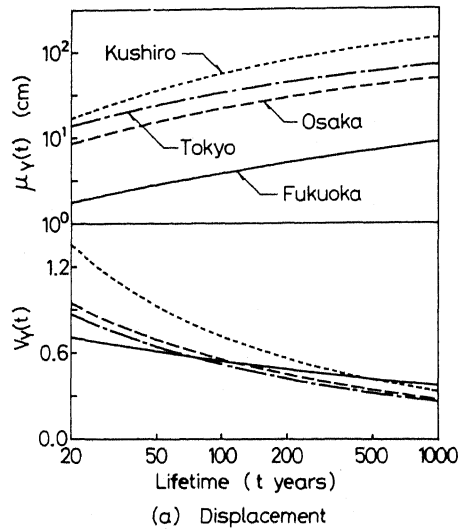


Fig. 6 Mean, μ_Y , and coefficient of variation, V_Y , of peak ground motions for the lifetime of t years

Table 2. Three parameters in the type III distribution

$$G_Z(z) = \exp \left[- \left(\frac{\log(w) - z}{\log(w) - \log(u)} \right)^k \right]$$

site		k	u	w
Fukuoka	dis.	6.98	0.155	79
	vel.	6.20	0.452	91
	acc.	5.96	2.748	236
Osaka	dis.	3.69	0.164	121
	vel.	4.23	0.683	99
	acc.	4.32	3.231	258
Tokyo	dis.	3.68	0.328	167
	vel.	3.36	0.753	110
	acc.	3.21	4.063	258
Kushiro	dis.	3.41	0.085	399
	vel.	3.66	0.564	283
	acc.	3.94	3.653	552

k : shape parameter

u : location parameter

w : upper limit

dis. : displacement (cm)

vel. : velocity (kine)

acc. : acceleration (gal)

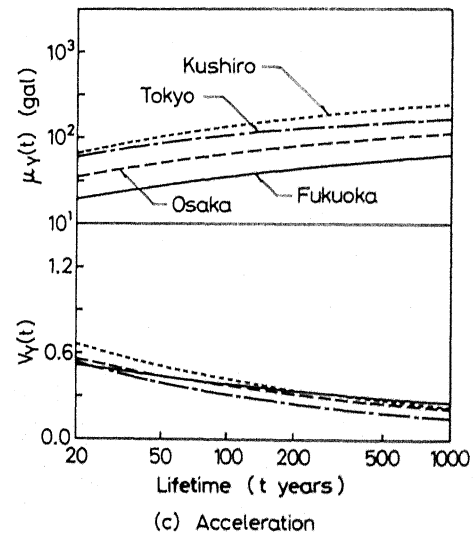


Table 3. Coefficients of variation of response amplification factor, F , after Mohraz et al. and peak ground motion, P , and peak response, R , in terms of 100-year lifetime maximum values

	COV of P	COV of F damping		COV of R lightly damped
		2%	5%	
displacement	60%	49%	46%	70%
velocity	45	45	40	60
acceleration	40	32	27	50